JPP JOURNAL OF Pharmacy and Pharmacology
ROYAL PHARMACEUTICAL SOCIETY
JPP Journal of Pharmacy And Pharmacology
Research Paper

Synthesis and plasma pharmacokinetics in CD-1 mice of a 18β-glycyrrhetinic acid derivative displaying anti-cancer activity

Benjamin Lallemand[a], Moustapha Ouedraogo[e], Nathalie Wauthoz[b], Touria Lamkami[a], Veronique Mathieu[c], Ivan Jabin[d], Karim Amighi[b], Robert Kiss[c], Jacques Dubois[a] and Jonathan Goole[b]

[a]Laboratory of Bioanalytical Chemistry, Toxicology, and Applied Chemistry, [b]Laboratory of Pharmaceutics and Biopharmaceutics, [c]Laboratory of Toxicology, Faculty of Pharmacy, and [d]Laboratory of Organical Chemistry, Faculty of Sciences, Université Libre de Bruxelles (U.L.B), Brussels, Belgium and [e]Laboratory of Pharmacology and Toxicology, Unit Training and Research in Health Sciences, Université de Ouagadougou, Ouagadougou, Burkina Faso

Keywords
cancer; glycyrrhetinic acid derivatives; mouse; nanoemulsion; plasma pharmacokinetics

Correspondence
Benjamin Lallemand, Laboratoire de Chimie BioAnalytique, Toxicologie et Chimie Physique Appliquée; Faculté de Pharmacie; Université Libre de Bruxelles (ULB); Bd du Triomphe; CP 205/01; 1050 Brussels; Belgium.
E-mail: benjamin.lallemand@ulb.ac.be

Received June 25, 2012
Accepted September 21, 2012

doi: 10.1111/j.2042-7158.2012.01603.x

Abstract

Objectives The plasma pharmacokinetic profile in CD-1 mice of a novel 18β-glycyrrhetinic acid (GA) derivative, which displays *in vitro* anti-cancer activity, was assessed.

Methods This study involved an original one-step synthesis of *N*-(2-{3-[3,5-bis(trifluoromethyl)phenyl]ureido}ethyl)-glycyrrhetinamide, (**2**) a compound that displays marked anti-proteasome and anti-kinase activity. The bioselectivity profile of **2** on human normal NHDF fibroblasts vs human U373 glioblastoma cells was assessed. Maximal tolerated dose (MTD) profiling of **2** was carried out in CD1 mice, and its serum pharmacokinetics were profiled using an acute intravenous administration of 40 mg/kg body weight.

Key findings Compound **2** displayed IC_{50} *in vitro* growth inhibitory concentrations of 29 and 8 μM on NHDF fibroblasts and U373 glioblastoma cells, respectively, thus a bioselectivity index of ~4. The intravenous pharmacokinetic parameters revealed that **2** was rapidly distributed ($t_{1/2dist}$ of ~3 min) but slowly eliminated ($t_{1/2elim}$ = ~77 min).

Conclusions This study describes an original and reliable nanoemulsion of a GA derivative with both anti-proteasome and anti-kinase properties and that should be further tested *in vivo* using various human xenograft or murine syngeneic tumour models with both single and chronic intravenous administration.

Introduction

The *in vitro* anti-cancer activity of 18β-glycyrrhetinic acid (GA) is well documented.[1–3] In addition, various GA derivatives display higher *in vitro* anti-cancer activity than GA itself,[4] and their mechanisms of action include pro-apoptotic,[5] antiproliferative[6] and anti-angiogenic[7] activity, among others. Several GA derivatives also target mitochondrial membrane permeability[8] and downregulate H-Ras activity[9] and beta-actin protein expression[10] in cancer cells. We recently synthesized a novel GA derivative, the *N*-(2-{3-[3,5-bis(trifluoromethyl)phenyl]ureido}ethyl)-glycyrrhetinamide (**2**), for which we demonstrated marked anti-proteasome and anti-kinase activity.[11]

The poor solubility of GA in water (<0.001 mg/ml) limits its bioavailability.[12] A lipidic nanoemulsion was developed as a suitable strategy with which to enhance the dissolution of both GA and its more lipophilic derivatives.[13] The main other GA derivatives developed in the anti-cancer field have only had their pharmacological properties explored.[7,14] Nowadays the pharmacokinetic profile of a potent anti-cancer drug is an important component of chemotherapeutics drug discovery and development.[15]

To evaluate the potential feasibility of delivering **2** via the intravenous route, we first developed an innovative lipophilic nanoemulsion formulation of this compound.

After profiling the nanoemulsion in terms of maximum tolerated dose (MTD) indices in healthy mice, a plasma pharmacokinetic study was conducted. A more straightforward chemical synthesis of **2** was also developed to obtain maximal yields of **2**. A simple and rapid HPLC method was also developed and validated to determine the concentration of **2** in organic or biologic fluids. This study evaluates the plasma pharmacokinetic behaviour of a synthetic derivative of GA (i.e. compound **2**) according to the physicochemical properties of this compound compared with the original molecule (i.e. GA).

Materials and Methods

General chemistry

Before their use, the solvents were distilled and dried using standard methods (i.e. tetrahydrofuran (THF) from Na/benzophenone, $CHCl_3$ from P_2O_5). The ^1H NMR spectra were recorded on a BRUKER AVANCE 300 (Brucker, Wissembourg, France) spectrometer in $CDCl_3$ using the residual isotopic solvent as reference for $\delta_H = 7.26$ ppm. The following abbreviations are used for spin multiplicity: s, singlet; t, triplet; m, multiplet; br, broad. Routine thin-layer chromatography (TLC) was performed on silica gel plates (Silica gel GF254 from VWR, Leuven, Belgium), and visualization was performed using UV. Flash column chromatography was carried out using silica gel at moderate pressure (spherical particle size 60–200 μm from MP Biomedicals, Brussels, Belgium). All reagents for the synthesis were obtained from Sigma-Aldrich (Bornem, Belgium). Solvent-grade reagents that were used for HPLC separation and measurements were purchased from ChemLab (Zedelgem, Belgium). The internal standard (I.S.) was a known compound that was synthesized by methylation of its carboxylic group by diazomethane[16] followed by oxidation of the alcohol function of 18β-GA by Jones reagent.[14] Water was de-ionized and purified with a Milli-Q system (Millipore, Overijse, Belgium).

Synthesis of *N*-(2-{3-[3,5-bis(trifluoromethyl) phenyl]ureido}ethyl)-glycyrrhetinamide (2)

The synthesis of compound **2** is shown in Figure 1. Ethylenediamine (13.10 ml, 195.99 mmol) was dissolved in 150 ml of anhydrous chloroform. A solution of 3,5-bis(trifluoromethyl)phenyl isocyanate (5.00 g, 19.59 mmol) in 80 ml of anhydrous chloroform was added dropwise at room temperature for 2 h and the reaction mixture was stirred for 24 h. After concentration under vacuum, the resulting residue was then dissolved in CH_2Cl_2, washed with 5×10 ml of brine, dried over Na_2SO_4, filtered and concentrated to produce the corresponding amine **1** (1.741 g, 28% yield). It is noteworthy that compound **1** was previously described in the literature, although it was obtained by a different procedure.[17] ^1H NMR (300 MHz, $CDCl_3$): δ (ppm) = 9.15 (brs, 1H, ArNH), 7.81 (s, 2H, ArH), 7.42 (s, 1H, ArH), 6.24 (brs, 1H, N*H*CH_2), 3.31 (m, 2H, C*H*$_2$$CH_2NH_2$), 2.93 (t, 2H, $J = 5.4$ Hz, C*H*$_2$$NH_2$).

18β-GA (1.00 g, 2.12 mmol) was solubilized in 20 ml of anhydrous THF. N,N'-dicyclohexylcarbodiimide (0.877 g, 4.25 mmol), 1-hydroxy-1*H*-benzotriazole (0.431 g, 3.19 mmol) and diisopropylethylamine (0.928 ml, 12.75 mmol) were added successively to the reaction mixture. After 10 min of stirring, the solution was cooled at 0°C, and a solution of the primary amine **1** (1.172 g, 3.71 mmol) dissolved in 5 ml of anhydrous THF was added dropwise. The reaction mixture was then stirred overnight at room temperature. The reaction mixture was concentrated under vacuum, and water (20 ml) was added. After dichloromethane extraction (3×20 ml), the organic layer was dried over anhydrous Na_2SO_4, filtered and concentrated under vacuum. N,N'-dicyclouracil was eliminated by precipitation in acetonitrile. The filtrate was evaporated under vacuum and the resulting crude product was then purified by flash column chromatography on silica gel (CH_2Cl_2; MeOH). The resulting residue was finally dissolved in CH_2Cl_2 and the solution was filtered. After concentration of the filtrate, **2** (1.512 g, 93% yield) was obtained as a white

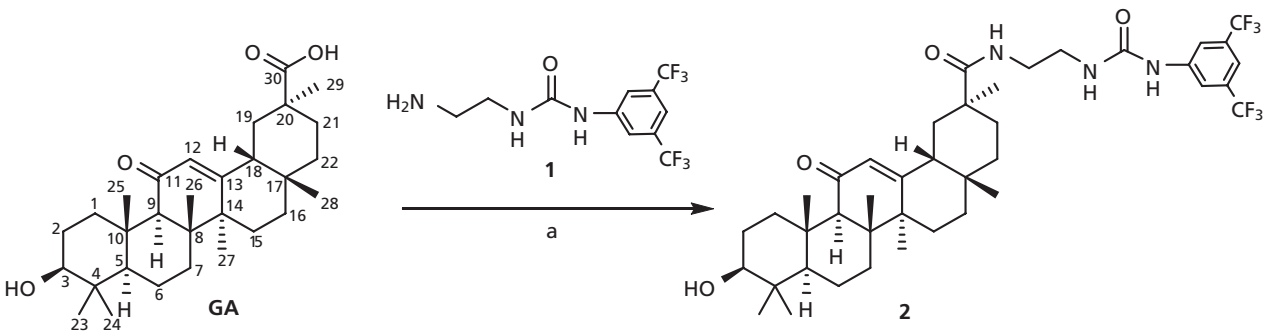

Figure 1 Reaction scheme for the synthesis of compound **2**. a: Tetrahydrofuran, N,N'-dicyclohexylcarbodiimide, 1-hydroxy-1*H*-benzotriazole, diisopropylethylamine, room temperature, 24 h, 93%.

solid. $R_f = 0.30$ (CH_2Cl_2; MeOH 95:5). The ^1H NMR data obtained for compound **2** are identical to those previously described in the literature.[11]

Oil-in-water nanoemulsion

Due to its physicochemical properties (e.g. high molecular weight, high lipophilicity) which are expected to limit its solubility in blood circulation, **2** was dissolved in oil, which was emulsified to obtain droplets characterized by a mean diameter of less than 1 μm (Figure 2). The selection of the oil is detailed in the Results section. Lecithin was used as the surfactant due to its US Food and Drug Administration (FDA)-approved status for intravenous administration (Table 1). Glycerol was added to reach physiological osmotic pressure. Both the aqueous and lipophilic phases were heated to 60–65°C before the emulsifying step. After complete dissolution of the components, the lipophilic phase was added to the aqueous solution under magnetic stirring (1500 rpm). The emulsion was homogenized using an Ultra-Turrax (IKA T-25; Janke & Kunkel, Staufen, Germany) with a rotational speed set at 24 000 rpm for 30 min in an ice-water bath. The mean diameter of the droplets was decreased with a high-pressure homogenizer (HPH; Emulsiflex-C5, Avestin, Ottawa, ON, Canada). The initial pressure was fixed at 5000 psi for 3 min, followed by 20 000 psi for 20 min. The homogenized dispersion was continuously cooled at 5°C during the entire process of size reduction. The size distribution of the droplets was measured in triplicate in liquid form with a Mastersizer 2000 laser diffractometer (Hydro 2000; Malvern Instruments, Worcester, UK) with a suitable standard operating procedure (refractive index 1.52, measurement time 30 s, 500 rpm).

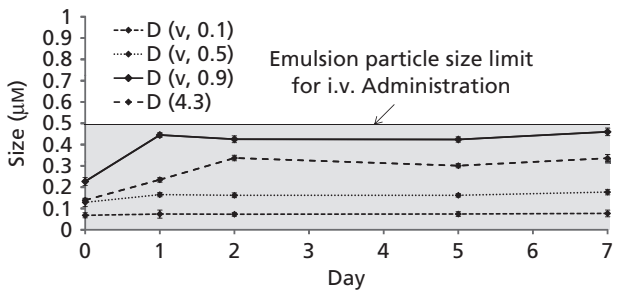

Figure 2 Particle size distribution of the nanoemulsion and stability over one week. D (v, 0.1) corresponds to 10% of the volume distribution that is below the indicated value and D (v, 4.3) represents the mean diameter of the nanoemulsion sample ($n = 3$).

Table 1 Compound **2** nanoemulsion composition

Component	% (m/v)
Oil phase	
Purified soybean oil	10
Lecithin (Lipid E80/S100)	1.2
Water phase	
Glycerol	2.25
Sodium oleate	0.03
Water	to 100

Description of the oil-in-water nanoemulsion preparation and its composition before the emulsifying step at 60–65°C.

Chromatographic conditions and validation of the bioanalytical method

The HPLC system consisted of an Agilent 1100 series (Agilent, Diegem, Belgium). The chromatographic system was a Chromolith performance RP-18 endcapped (4.6 mm × 100 mm) (Merck, Darmstadt, Germany) using the mobile phase as follows: MeOH : water (80:20, v/v) (0.01% TFA) for 8 min. The detection system was an Agilent Diode Array Detector G1315B. The chromatogram was measured by this HPLC method at 249 nm, and it was run at an isocratic flow rate of 2.0 ml/min through the column to elute the analyte. The data integration was carried out with Chemstation software. Calibration curves were prepared using plasma samples spiked with **2** at a final plasma concentration of 2, 5, 10, 20, 50, 100 and 250 μg/ml, and a single injection was used for each of three calibration standards curves and four validation standards curves each day. After 3 days, the results were analysed with the validation approach previously published by Hubert *et al.*,[18] which is in agreement with the procedures recommended by the FDA, bioanalytical method validation guidance, ICH documents and Washington conference.[18]

In vitro growth inhibitory assessment

The IC_{50} *in vitro* growth inhibitory concentrations of **2** was determined by means of the MTT colorimetric assay in human U373 glioblastoma cells (European Collection of Cell Culture, ECACC code 89081403, Salisbury, UK) and human NHDF fibroblasts (PromoCell C-12300, Heidelberg, Germany) after three days of cell culture with **2**.

The assay was performed previously described.[11] Six data points were available for each concentration tested and nine concentrations from 0.01 to 100 μM were available for each cell line (Figure 3).

Animal study, plasma collection and extraction

Six-week-old female CD1 mice (Charles Rivers, Arbresle, France), 18–22 g, were used and the experiment was performed on the basis of authorization no. LA 1230568 from the Animal Ethics Committee of the Federal Department

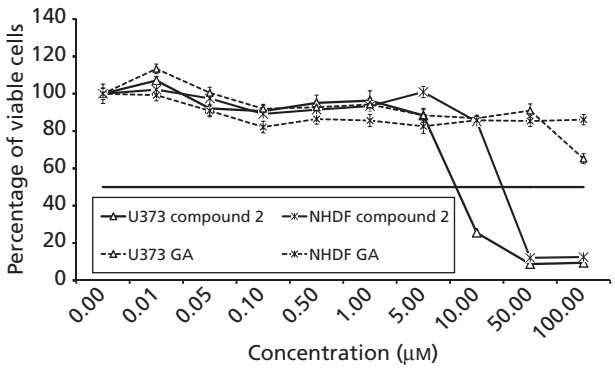

Figure 3 *In vitro* growth inhibitory assessment of compound **2** and GA on different normal (fibroblasts NHDF) and cancer (glioblastoma U373) cells to determine bioselectivity by means of their half maximal inhibitory concentration (IC_{50}) determination. Each data point is represented by mean ± SEM ($n = 6$).

of Health, Nutritional Safety, and the Environment (Belgium). Mice were housed at 22–25°C in a protected environment with free access to food and water according to ethics guidelines.

The appropriate dose for the plasma bioavailability assessment was first evaluated by screening chronic doses administered intravenously (in a final volume of 200 µl) of 10–80 mg/kg into the vein tail of female CD-1 mice, an assessment that was defined as the maximal tolerated dose (MTD) index. The nanoemulsion vehicle alone was also administered to healthy mice to analyse the potential toxicity of this formulation. The vehicle alone or the vehicle containing **2** was injected intravenously three times a week (Monday, Wednesday and Friday) for three consecutive weeks. The survival and behaviour of each mouse were monitored for 19 days following the last of the nine intravenous injections.

The determination of the MTD index led to use of 40 mg/kg of **2** in the nanoemulsion, equivalent to the MTD/2 (see the Results section), in the plasma pharmacokinetic study. This dose was administered intravenously to healthy mice. At predetermined post-injection time points (5, 15, 30, 60, 120 min and 3 h), mice were injected with a lethal dose of Nembutal (intraperitoneal administration) to collect the maximal blood volume by intracardiac puncture. Blood samples were then immediately centrifuged at 3000*g* for 10 min. All plasma samples (four mice at each time point) were stored at –20.0°C until analysis.

Each plasma sample (100 µl) was transferred to a 0.5 ml Eppendorf tube containing 10 µl of methylated and oxidized GA (I.S.) at 0.5 mg/ml. To precipitate proteins and to extract **2** and the I.S. from the plasma samples, 190 µl of methanol was added and mixed for 20 min before centrifugation at 10 000*g* for 15 min. The supernatant was then collected, and 50 µl was injected into the HPLC system.

Statistical analysis

Statistical comparisons were made by the Kruskal–Wallis test (a nonparametric one-way analysis of variance). Where this test revealed significant differences, treatment groups were then compared by applying the Mann–Whitney *U*-test. When the number of experiments was less than $n = 4$, the mean ±SD was used. The statistical analysis was performed using Statistica software (Statsoft, Tulsa, OK, USA).

Results

Synthesis of compound 2

The synthesis of compound **2** was previously described according to a three-step strategy with an overall 36% yield.[11,19] A one-step synthesis of compound **2** was thus developed to (1) improve this moderate yield, (2) avoid arduous purification processes and (3) allow a multigramme-scale synthesis. The new strategy consisted of the direct reaction of GA with the known amino compound **1**[17] in the presence of peptide coupling agents (i.e. HOBT and DCC) (Figure 1). This straightforward strategy afforded **2** in an excellent 93% yield after a simple purification by flash chromatography on silica gel. The purity (99%, $R_t = 5.5$ min) of **2** was determined by a reverse HPLC system according to the chromatographic analyses described below. In addition to a further pharmaceutical quality insurance, a maximal purity was targeted to be consistent with the intravenous administration.

Preformulation study

A preformulation study was performed to characterize both the solubility and the calorimetric profile of **2**. The characterization of these physicochemical properties was relevant to select and optimize the technical process for the potential formulations for intravenous administration.[20] Briefly, the solubility profile of **2** was determined in different oils (cod liver oil, almond oil, soybean oil, corn oil) with an acceptance limit of solubility (5 mg/100 µl). Compound **2** was shown to be soluble in soybean oil, the only FDA-approved oil for intravenous administration. Therefore, a nanoemulsion formulation using soybean oil was set up to perform the *in vivo* plasma pharmacokinetic studies in mice.

The calorimetric profile of **2** in its solid state was assessed by thermogravimetric analyses and differential scanning calorimetry. To decrease the tensile strength at the interface during the formation of the emulsion, the emulsification process required an elevation of temperature to 60–65°C in both phases. The thermogravimetric measurements demonstrated that the thermal degradation of **2** appeared to begin

at approximately 200°C, which was appreciably higher than the temperature needed during the emulsification process reported above.

The nanoemulsion containing **2** was used to perform the *in vivo* plasma pharmacokinetic study in mice.

Nanoemulsion particle size and stability

The initial emulsion was performed using an Ultra-Turrax apparatus to disperse the generated droplets. However, their mean diameter was not suitable for intravenous administration, as it reached 8.95 μm. Therefore, a further step was introduced to improve both the size distribution and the mean diameter d(4.3). A high-pressure homogenization process decreased the mean diameter of the dispersed droplets to the nano range (e.g. 140 nm). The stability of the size distribution was evaluated after 1, 2, 5 and 7 days post formulation. The stability of the emulsion was assessed before performing the *in vivo* study because the same stock standard dispersion was used for all of the *in vivo* experiments. The dispersions were maintained at 4°C and, as seen in Figure 2, the mean diameter d(4.3) of the droplets contained in the stock standard emulsion remained in the nanoscale for at least one week, which corresponded to the period allotted for the experimental protocol. Moreover, chromatographic analyses with 99% peak area recovery confirmed the absence of degradation for compound **2** after the 7 days of analyses.

In vitro bioselectivity of compound 2

Our previous study[11] demonstrated mean *in vitro* growth inhibition values for **2** of about 7 μM in eight distinct cancer cell lines. The percentages of viable normal NHDF fibroblasts and U373 glioblastoma cells in the presence of compound **2** and GA are illustrated in Figure 3. The *in vitro* growth inhibition concentration was 8 μM for U373 glioblastoma cells, while it increased to 29 μM for NHDF fibroblasts. This means that compound **2** displays a bioselectivity index of ~4 *in vitro*. The bioselectivity profile of GA was not determined because its IC_{50} *in vitro* growth inhibitory concentration was greater than 50% (Figure 3). We did not assay GA derivatives other than compound **2** from our novel series because we previously demonstrated that only compound **2** (labelled compound **6b** in our previous study) was able to inhibit the proteasome activity (on the three catalytic sites) without inhibiting peroxisome proliferator-activated receptor (PPAR)γ activity.[11]

Maximum tolerated dose

The MTD profiles were established by weighing mice every two days from day 1 to day 40 (Figure 4). The mice injected intravenously with 80 mg/kg displayed slight weight loss, a feature that could relate to the presence of some toxic effects. The mice in the control group, which received the vehicle only, displayed no apparent signs of toxicity. The statistical analyses revealed significant differences between the control or 40 and 80 mg/kg-treated groups when using compound **2** (Mann–Whitney *U*-test, $P < 0.001$), but not between the control and the 40 mg/kg group ($P > 0.05$). Consequently, a dose of 40 mg/kg was selected to assess the *in vivo* plasma pharmacokinetic profile of **2** in CD1 mice.

We paid attention to compound **2** only for the following reasons. First, as argued in our previous study,[11] we wanted to synthesize novel GA derivatives with the specific aims of developing novel proteasome inhibitors, with inhibitory effects on the three catalytic sites. As we knew from the literature that some GA derivatives can modulate PPAR activity, we also wanted to be sure that the GA derivatives that we synthesized do not affect PPAR activity, and more precisely do not inhibit PPARγ activity. Only compound **2** fitted in with all our goals as detailed previously.[11]

Validation of the bioanalytical method

The accuracy profile was obtained according to the method described by Hubert *et al*.[18] and is illustrated in Figure 5. The limit of quantification (LOQ) was determined as the intersection of the relative error curve and the maximum tolerated error line fixed for biological batches in complicated matrix, which is 30%. LOQ was measured at 3.4 μg/ml plasma and the limit of detection (LOD) was observed at 1 μg/ml (Figure 5).

In vivo plasma pharmacokinetic profile of compound 2

The pharmacokinetic profile relating to the intravenous administration of **2** allows various parameters to be calculated as detailed in Table 2. These parameters were evaluated by means of the FADHA program using the algorithm developed by Abikhalil *et al*.[21] The two-compartment modelling takes into account a weighting function of $1/C_i^2$ (concentration at i time) and all errors that could appear during the experiment (i.e. the fact that each batch time corresponds to only one mouse, in contrast with human pharmacokinetics, where one batch time always comes from the same human). The curve profile (Figure 6) was minimized, conferring greater accuracy and precision in the estimation of the pharmacokinetic parameters with the best exponential curves conducted with the minimal residual least square sum. The first four identified parameters (A1, A2, a1, a2) were determined to generate the formula detailed in Table 2. From these data the secondary parameters were recalculated from the identified parameters. The exposition level of **2** was expressed by the area under the curve (AUC) and the C_{max} (maximal concentration

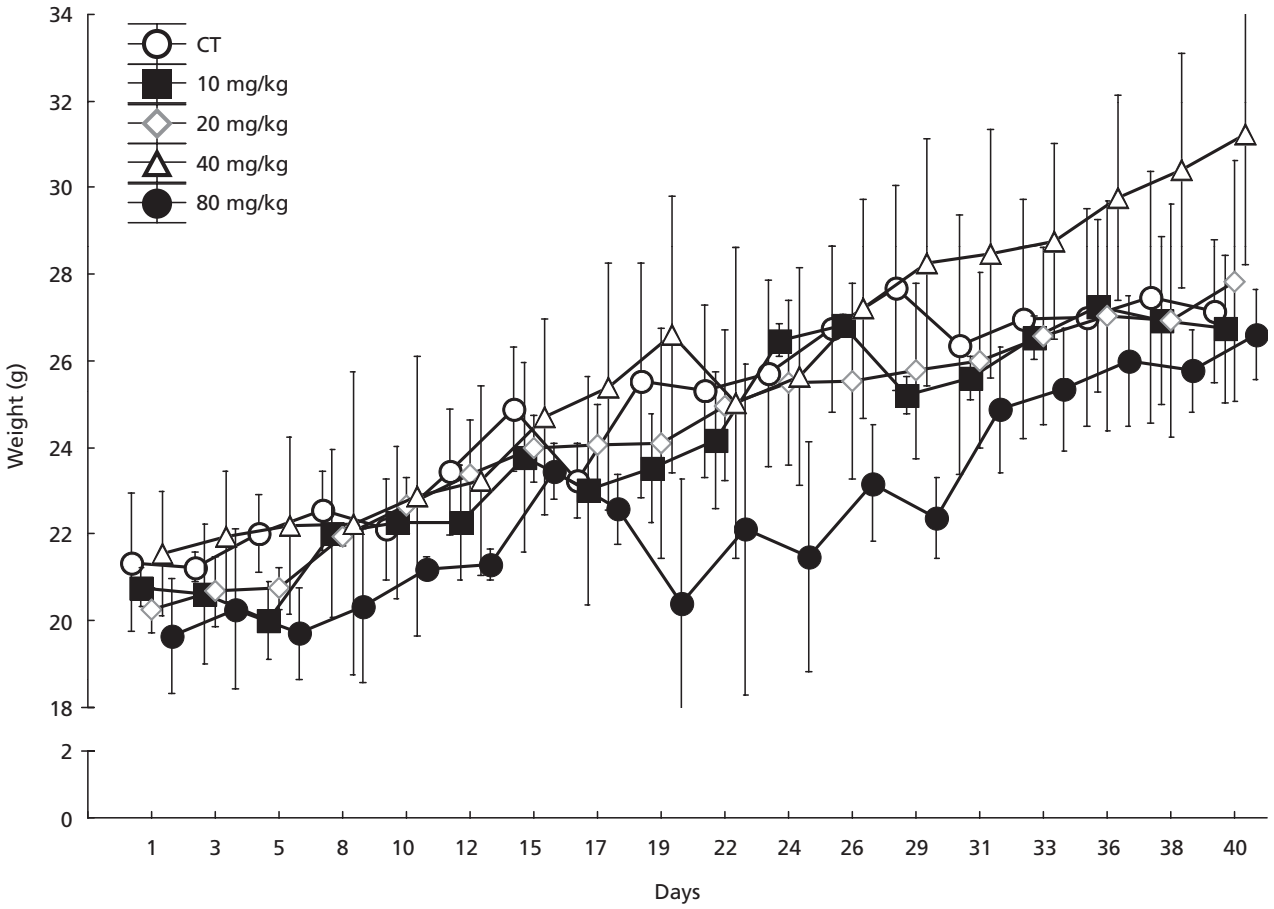

Figure 4 Maximum tolerated dose evaluated by the establishment of the weight curve after multiple intravenous injections. The control group received the nanoemulsion vehicle in the same injection volume. Each data point is represented by mean ± SD ($n = 3$).

Table 2 Pharmacokinetic parameters of compound **2**

$C_t = A_1\ e^{-a1t} + A_2\ e^{-a2t}$		
Parameters	FADHA recalculated value	Units
A1	251.39 ± 0.07	µg/ml
A2	8.38 ± 0.07	µg/ml
a1	0.228 ± 0.009	min^{-1}
a2	0.0089 ± 0.0001	min^{-1}
t_{max}	0.02	min
C_{max}	259.8	µg/ml
AUC	2034.6	µg min/ml
Cl	0.0004	ml/min
$t^1/_{2dist}$	3.03	min
$t^1/_{2elim}$	77.27	min

Pharmacokinetic parameters determined by the FADHA program for intravenous administration of compound **2** at 40 mg/kg.

estimated in blood circulation). In contrast, the half-life and clearance represented the elimination parameters comprising the metabolism and excretion of compound **2**. The initial rapid decline of the intravenous concentration route suggests that the majority of the drug is distributed to peripheral compartments with a distribution $t_{1/2dist}$ of 3.03 min. Nevertheless, the second parameter revealed that **2** was not directly eliminated ($t_{1/2elim} = 77.27$ min) (Table 2, Figure 6).

Discussion

The non-regulatory preclinical development of a new potential chemotherapeutic drug, particularly in oncology, requires at least the optimization of the chemical synthesis, characterization of its physicochemical properties, and appropriate formulation at non-toxic *in vivo* doses, thus preliminary toxicological analyses.[15] In addition, the plasma pharmacokinetic behaviour of the compound of interest is also an important component for further demonstration of *in vivo* anti-cancer activity in various rodent tumour models including syngeneic and xenograft models. This study thus assessed the plasma pharmacokinetic profile at non-toxic concentration (i.e. 40 mg/kg via the intravenous route) of a new 18β-GA derivative, compound **2**, for

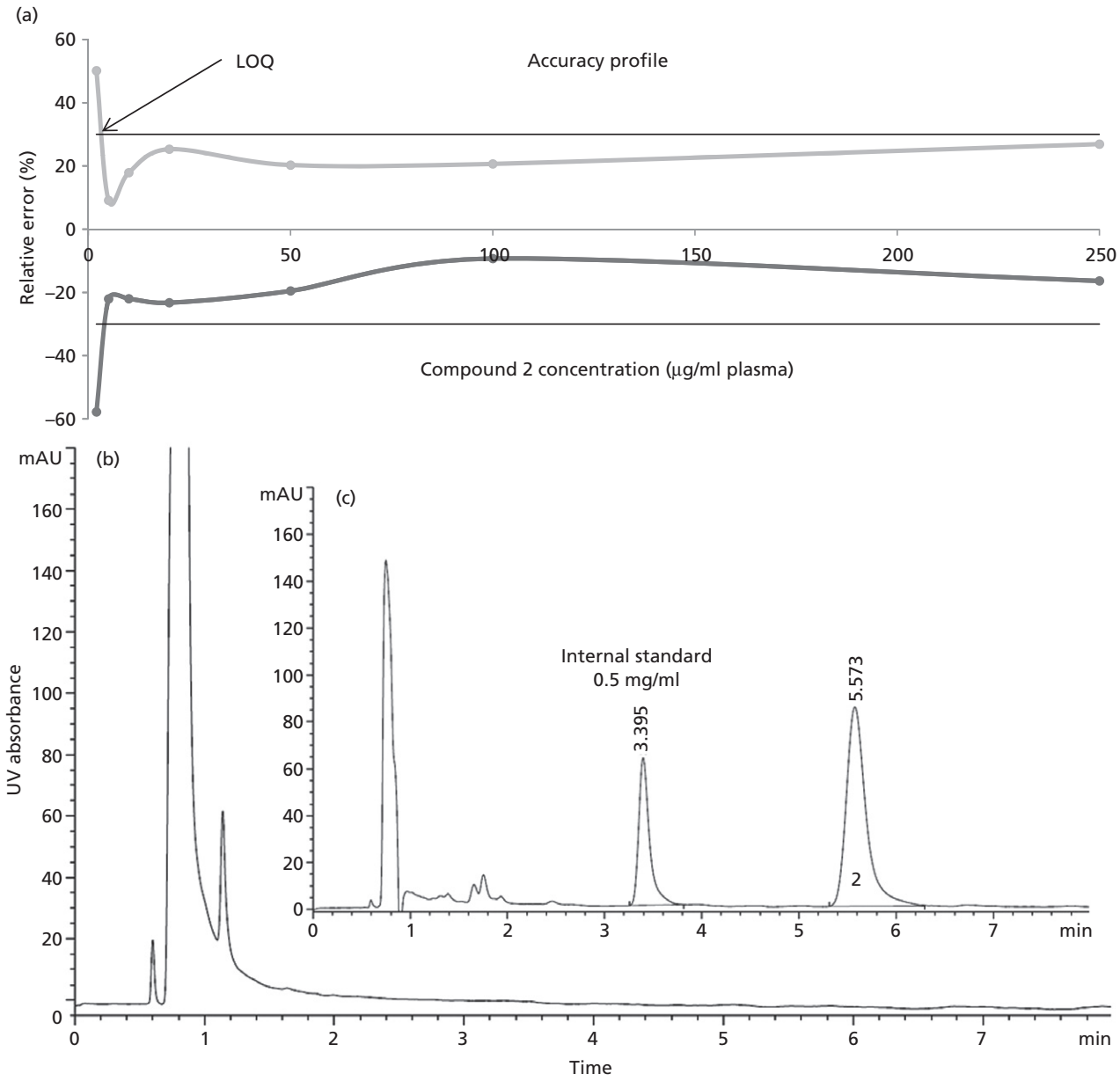

Figure 5 (a) Accuracy profile for the quantification of compound **2** in plasma. (b) Chromatogram of free plasma extracted from CD1 mouse. (c) Chromatogram of plasma extracted with the internal standard from CD1 mice that received compound **2** intravenously at 40 mg/kg after 5 min.

which we previously demonstrated both anti-proteasome and anti-kinase activity.[11] The pharmacokinetic parameters obtained show that the plasma profile of compound **2** is associated with a rapid decline followed by a slow elimination as indicated by the respective $t_{1/2}$. A previous study already characterized the plasma pharmacokinetic profile of GA following the intravenous route of administration and reported a rapid distribution phase followed by a slower elimination phase,[22] a profile that therefore resembles the one reported here for **2**. It is worth noting that GA had been previously described to cross the brain–blood barrier,[23] a mechanism that could explain the fast decline of **2** in the distribution phase and will need to be verified in the future. This hypothesis could be investigated with the help of the newly radiosynthesized derivative of *N*-(2-{3-[3, 5-bis(trifluoromethyl)]phenyl[^{11}C]ureido}ethyl)-glycyrrhetinamide.[19] Therefore, due to its higher log P prediction compared with GA, to its *in vitro* bioselectivity and its

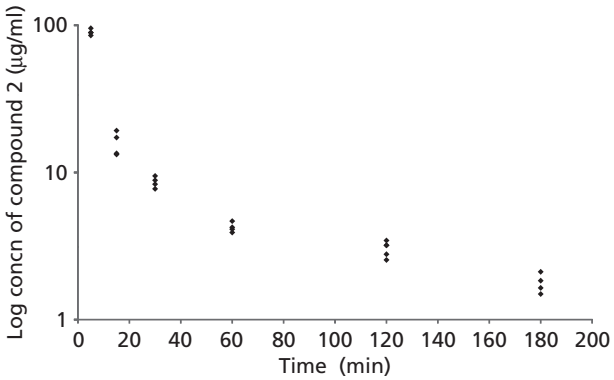

Figure 6 Pharmacokinetic profile of compound **2** after intravenous administration at 40 mg/kg in CD1 mice. Mean concentration of compound **2** from different mice ($n = 4$). The best resultant exponential equation was $C_t = 251.39\ e^{-0.228t} + 8.38\ e^{-0.0089t}$.

similar pharmacokinetic profile, compound **2** represents an interesting candidate for further studies focusing on the distribution of **2** in brain with the aim of combating various brain cancers.

Conclusions

The data obtained in this study reveal that compound **2**, a novel GA derivative with marked anti-proteasome activity,[11] can be synthesized in one step with a yield > 90%. The *in vitro* growth inhibitory levels of compound **2** on normal cells compared with cancer cells indicate an interesting bioselective effect. A nanoemulsion formulation of this compound enables *in vivo* delivery through intravenous administration to healthy mice with a pharmacokinetic profile that reveals a wide distribution and a low elimination rate similar to the profile of GA. The nanoemulsion that we have developed is therefore suitable for future *in vivo* analyses of compound **2**-related anti-cancer activity.

Declarations

Conflict of interest

The Author(s) declare(s) that they have no conflict of interest to disclose.

Funding

This research received no specific grants from any funding agency in the public, commercial or not-for profit sectors.

Acknowledgements

Robert Kiss is a Director of Research with the Fonds National de la Recherche Scientifique (FNRS, Belgium). We thank all the members of the Laboratory of Toxicology who helped us with respect to the *in vivo* plasma pharmacokinetic experiments. We also thank F. Wolff and F. Cotton from the Department of Medical Chemistry (Erasme Hospital, Brussels) for their help in the validation of the bioanalytical methods.

References

1. Abe H *et al*. Effects of glycyrrhizin and glycyrrhetinic acid on growth and melanogenesis in cultured B16 melanoma cells. *Eur J Cancer Clin Oncol* 1987; 23: 1549–1555.
2. Okamoto H *et al*. Inhibition of 12-Otetradecanoylphorbol-13-acetate-induced induction in Epstein-Barr virus early antigen in Raji cells. *Cancer Lett* 1983; 19: 47–53.
3. Gao Y *et al*. The synthesis of glycyrrhetinic acid derivatives containing a nitrogen heterocycle and their antiproliferative effects in human leukemia cells. *Molecules* 2010; 15: 4439–4449.
4. Lallemand B *et al*. Structure-activity relationship analyses of Glycyrrhetinic acid derivatives as anticancer agents. *Mini Rev Med Chem* 2011; 11: 881–887.
5. Salvi M *et al*. Glycyrrhetinic acid-induced permeability transition in rat liver mitochondria. *Biochem Pharmacol* 2003; 66: 2375–2379.
6. Subba Rao GSR *et al*. Chemical modifications of natural triterpenes-glycyrrhetinic and boswellic acids: evaluation of their biological activity. *Tetrahedron* 2008; 64: 11541–11548.
7. Pang X *et al*. Methyl 2-cyano-3,11-dioxo-18-olean-1,12-dien-30-oate, a derivative of glycyrrhetinic acid, functions as a potent angiogenesis inhibitor. *J Pharmacol Exp Ther* 2010; 335: 172–179.
8. Lee CS *et al*. 18beta-Glycyrrhetinic acid induces apoptotic cell death in SiHa cells and exhibits a synergistic effect against antibiotic anti-cancer drug toxicity. *Life Sci* 2008; 83: 481–489.
9. Yu T *et al*. Selective cytotoxicity of glycyrrhetinic acid against tumorigenic r/m HM-SFME-1 cells: potential involvement of H-Ras downregulation. *Toxicol Lett* 2010; 192: 425–430.
10. Yamaguchi H *et al*. Novel effects of glycyrrhetinic acid on the central nervous system tumorigenic progenitor cells: induction of actin disruption and tumor cell-selective toxicity. *Eur J Med Chem* 2010; 45: 2943–2948.
11. Lallemand B *et al*. *N*-(2-{3-[3,5-bis(trifluoromethyl)phenyl]ureido} ethyl)-glycyrrhetinamide (6b): a novel anticancer Glycyrrhetinic acid derivative that targets the proteasome and displays anti-kinase activity. *J Med Chem* 2011; 54: 6501–6513.
12. Lu Y *et al*. In vitro and in vivo evaluation of mPEG-PLA modified liposomes loaded glycyrrhetinic acid. *Int J Pharm* 2008; 356: 274–281.
13. Hao J *et al*. Effect and mechanism of penetration enhancement of organic base and alcohol on Glycyrrhetinic

acid in vitro. *Int J Pharm* 2010; 399: 102–108.
14. Logashenko EB *et al*. Synthesis and pro-apoptotic activity of novel glycyrrhetinic acid derivatives. *ChemBioChem* 2011; 12: 784–794.
15. Gad SC. *Preclinical development handbook: ADME and biopharmaceutical properties*. Hoboken, NJ: John Wiley and sons, 2008.
16. Ignatov DV *et al*. A simple method for preparation of 18 alpha-glycyrrhetinic acid and its derivatives. *Russ J Bioorganic Chem* 2003; 29: 390–394.
17. Park JH, Oh CH. Synthesis of new 6-(-4-fluorophenyl)-5-(2-substituted pyrimidin-4- yl)imidazo[2,1-b] thiazole derivatives and their antiproliferative activity against melanoma cell line. *Bull Korean Chem Soc* 2010; 31: 2854–2860.
18. Hubert P *et al*. Harmonization of strategies for the validation of quantitative analytical procedures. A SFSTP proposal-Part III. *J Pharmaceut Biomed* 2007; 45: 82–96.
19. Asakawa C *et al*. Utilization of [11C]phosphogene for radiosynthesis of *N*-(2-{3-[3,5-bis(trifluoromethyl) phenyl[11C]ureido}ethyl)-glycyrrhetinamide, an inhibitory agent for proteasome and kinase in tumors. *Bioorg Med Chem Lett* 2012; 22: 3594–3597.
20. Li P, Zhao L. Developing early formulations: practice and perspective. *Int J Pharm* 2007; 341: 1–19.
21. Abikhalil F *et al*. A new algorithm for computing the parameters of linear compartment models in pharmacokinetics. *Eur J Drug Metab Pharmacokinet* 1986; 11: 51–59.
22. Krähenbühl S *et al*. Analysis and pharmacokinetics of glycyrrhizic acid and glycyrrhetinic acid in humans and experimental animals. *Steroids* 1994; 59: 121–126.
23. Tabuchi M *et al*. The blood-brain barrier permeability of 18 beta-glycyrrhetinic acid, a major metabolite of glycyrrhizin in Glycyrrhiza root, a constituent of traditional Japanese medicine yokukansan. *Cell Mol Neurobiol* 2012; 32: 1139–1146.